Indian J Pure Appl Math (2022) 53:813–825
https://doi.org/10.1007/s13226-021-00175-9

ORIGINAL RESEARCH

A new a priori estimation for singularly perturbed problems with discontinuous data

V. P. Ramesh · S. Janakiraman · M. Prithvi · G. Narayani

Received: 21 February 2021 / Accepted: 25 August 2021 / Published online: 27 September 2021

Abstract The main aim of this article is to present an a priori estimate of an exponential layer and thereby a new mesh (G-mesh) for a class of singularly perturbed problems with discontinuous data. We have also proved that the standard upwind scheme on the proposed mesh is parameter uniformly convergent and is of almost first order. To demonstrate the efficiency of the proposed mesh we carried out a few numerical experiments comparing the performance of the proposed G-mesh with other standard meshes available in the literature.

Keywords Singularly perturbed problem (SPP) · Interior layer · G-mesh · Finite difference scheme · B-type mesh · Shishkin mesh

Mathematics Subject Classification 34E15 · 34K28

1 Introduction

In this article, we consider the following class of singularly perturbed convection-diffusion problems [1] such that the solution exhibits a strong interior layer at the point of discontinuity of the convection coefficient.

$$
\begin{aligned}
L_\epsilon u(x) := \epsilon u''(x) + b(x)u'(x) &= f(x), \quad \forall x \in \Omega^- \cup \Omega^+, \\
u(0) = u_0, &\quad u(1) = u_1, \\
b(x) < -\alpha_1 < 0, \ \ x < d, &\quad b(x) > \alpha_2 > 0, \ \ x > d, \\
|[b](d)| \le C, &\quad |[f](d)| \le C,
\end{aligned}
\tag{1}
$$

where $0 < \epsilon \ll 1$ is the perturbation parameter, C is a positive arbitrary constant independent of ϵ, the domain $\Omega = (0, 1)$ and subdomains, $\Omega^- = (0, d)$, $\Omega^+ = (d, 1)$. The functions b, f are assumed to be twice

Communicated by G. D. Veerappa Gowda.

Supplementary Information The online version contains supplementary material available at https://doi.org/10.1007/s13226-021-00175-9.

V. P. Ramesh (✉) · M. Prithvi · G. Narayani
Mathematics and Analytics Center of Excellence (MACoE), Department of Mathematics, Central University of Tamil Nadu, Thiruvaur, India
E-mail: vpramesh@gmail.com

S. Janakiraman
Centre for Development of Advanced Computing (CDAC), Bengaluru, India
E-mail: jraman@cdac.in

continuously differentiable in $\Omega^- \cup \Omega^+$. Further, we assumed discontinuity at d and the jump discontinuity of some function ζ at d is given as $[\zeta](d) := \zeta(d^+) - \zeta(d^-)$.

Now, using the decomposition technique presented in [1], we decompose the solution of (1) as $u = y + z$, where y (smooth component) is the solution of

$$\begin{aligned} L_\epsilon y(x) &= f(x) \qquad \forall\, x \in \Omega^- \cup \Omega^+, \\ y(0) &= u(0), \qquad y(1) = u(1), \\ y(d^-) &= y_0(d^-) + \epsilon y_1(d^-), \quad y(d^+) = y_0(d^+) + \epsilon y_1(d^+) \end{aligned}$$

and z (singular component) is the solution of,

$$\begin{aligned} L_\epsilon z(x) &= 0 \quad \forall\, x \in \Omega^- \cup \Omega^+, \\ z(0) &= 0, \quad z(1) = 0, \\ [z](d) &= -[y](d), \qquad [z'](d) = -[y'](d). \end{aligned} \tag{2}$$

Further, y_0 and y_1 are chosen such that

$$\begin{aligned} a y_0' &= f(x), \quad x \in \Omega^- \cup \Omega^+, \quad y_0(0) = u(0),\ y_0(1) = u(1) \\ a y_1' &= -y_0'', \quad x \in \Omega^- \cup \Omega^+, \quad y_1(0) = 0,\ y_1(1) = 0 \end{aligned}$$

and $[y](d) = y(d^+) - y(d^-)$. Also, $y + z \in C^1(\Omega)$ and it is assured from the equation (2).

Using the above decomposition technique, Farell et al. had proved the following lemma which will be useful while presenting the analysis of the proposed algorithm.

Lemma 1 *For $0 \le k \le 4$, y (smooth component) and z (singular component) are bounded as follows,*

$$|y^{(k)}|_{\Omega^-} \le C(1 + \epsilon^{2-k}), \qquad |y^{(k)}|_{\Omega^+} \le C(1 + \epsilon^{2-k}),$$
$$|[y](d)| \le C, \qquad |[y'](d)| \le C, \qquad |[y''](d)| \le C \text{ and}$$
$$|z^k(x)| \le \begin{cases} C\, \epsilon^{-k} e^{-(d-x)\alpha_1/\epsilon} & \forall x \in \Omega^-, \\ C\, \epsilon^{-k} e^{-(x-d)\alpha_2/\epsilon} & \forall x \in \Omega^+. \end{cases}$$

This class of problems were discussed by Farrell et al. in 2004 where the authors developed an ϵ-uniformly convergent numerical algorithm on a piecewise uniform mesh namely Shishkin mesh [1]. In the same year, Farrell et al. [2] considered a similar class of problems with a discontinuous source term and had proved that the standard upwind algorithm on Shishkin mesh is ϵ-uniformly convergent. In 2004, O'Riordan and Shishkin [3] had analysed the convergence of implicit upwind scheme on Shishkin mesh for singularly perturbed parabolic differential equations with discontinuous convection coefficient and discontinuous source term. In 2005, Cen [4] presented the analysis of a hybrid finite difference scheme on Shishkin mesh for the considered class of problems (1). In 2011, Kaushik and Natesan had proposed a hybrid numerical method using Shishkin mesh [5] yielding an ϵ-uniformly convergent method to the class of problems considered by O'Riordan and Shishkin [3]. In 2011, Rai and Sharma [6] considered singularly perturbed differential-difference equations with interior layers and presented the analysis of modified El-Mistikawy-Werle scheme. In 2017, Cen et al. [7] had proposed a high-order scheme on Shishkin mesh for a similar class of problems with a discontinuous source term. In 2018, Ramesh et al. [8] had proposed a new a priori estimate and thereby a new mesh, namely $H(\ell)$ mesh for different class of problems. Furthermore, in 2020, Ramesh et al. [9] had proved the efficiency of upwind scheme on $H(\ell)$ mesh for the considered class of problems (1) and had proved that the standard upwind scheme on $H(\ell)$ mesh is parameter uniformly convergent. In 2020, Rai and Sharma [10] presented the analysis of upwind scheme on Shishkin mesh for a similar class of problems with a weak interior layer.

Vulanovic [11] presented a new a priori estimate modifying the idea of Bakhvalov [12] and the proposed non-uniform mesh is referred to as B-type mesh. It is not adapted by many researchers due to the complexity arising out of the non-uniformity in the distribution of mesh points in the layer region. It is not an exaggeration to mention that only a very few researchers have reduced this mesh to practice. Further, Vulanovic had proved that a finite different scheme is parameter uniformly convergent for a different class of problems and also emphasized the need for new a priori estimation of the exponential layer region. In this article, we present a new mesh based on an extension idea of harmonic mesh which we proposed in 2018 [8] and we present our detailed analysis and various experiments comparing the performance of standard upwind algorithm on the proposed mesh with other meshes in the literature namely, Shishkin, harmonic and B-type meshes.

An outline of this article is as follows: In Section 2, the construction of the proposed mesh (G-mesh) is presented. Section 3 provides the convergence analysis of the upwind scheme on the proposed G-mesh. Finally, numerical results are presented in Section 4 to show the parameter uniform convergence of the proposed algorithm. We have also presented a comparison study of upwind scheme on various meshes namely, Shishkin, harmonic and B-type meshes.

2 The proposed a priori estimation : G-mesh

In 2018, we proposed and proved the efficiency of harmonic mesh to capture the exponential layer behavior of the solution [8]. It is to be noted that our harmonic mesh was based on the arithmetic function $g : \mathbb{N} \setminus \{1\} \to \mathbb{R}$ and it is defined as

$$g(n) := \sum_{k=1}^{n-1} \frac{1}{k}$$

ignoring the harmonic $\frac{1}{n}$ [8,9]. In other words we found that set of harmonics $\{1, \frac{1}{2}, \ldots \frac{1}{n-1}\}$ which is a proper subset of $\{1, \frac{1}{2}, \ldots \frac{1}{n}\}$ was able to estimate the boundary layer on par with other meshes in the literature [8,9,11, 13,14]. We refer to [8] for asymptotic and analytic behavior of this harmonic function, namely g.

Our motivation was to generalize the above idea or at least to answer a special case of generalisation of harmonic mesh. In other words, we want to answer whether there exist any proper subset S of $\{1, \frac{1}{2}, \ldots \frac{1}{n}\}$ other than $\{1, \frac{1}{2}, \ldots \frac{1}{n-1}\}$ such that the arithmetic function $f : \mathbb{N} \setminus \{1\} \to \mathbb{R}$ defined as

$$f(n) := \sum_{k \in S} \frac{1}{k}$$

be able to capture the boundary layer like other meshes in the literature.

It is very natural to consider the prime harmonics which will be a proper subset of $\{1, \frac{1}{2}, \ldots \frac{1}{n}\}$, denoted by p as defined below and we found that it is not even close to any of these a priori estimates in the literature.

$$p(n) := \sum_{\substack{k=2 \\ k \text{ is prime}}}^{n} \frac{1}{k}$$

In this article, we propose a subset of $\{1, \frac{1}{2}, \ldots \frac{1}{n}\}$ using Gauss's theorem on primitive roots [21] and have also proved that it is efficient on capturing the exponential layer like other meshes in the literature. Gauss while studying the periods of rational numbers $1/p$ (where p is any prime number other than 2 and 5) when expressed in decimal system observed a connection between the periods of $1/p$ and the order of 10 in the multiplicative group modulo p. Gauss further proved that *the multiplicative group* $(\mathbb{Z}/k\mathbb{Z})^*$ *is cyclic if and only if* $k = 2, 4, p^\ell$ *or* $2p^\ell$ *for all odd primes* p *and for all positive integers* ℓ. We consider the harmonic $\frac{1}{k}$ if k is 2 or 4 or is of the form p^k or $2p^k$, where p is any odd prime and $\ell \in \mathbb{N}$, in other words, we consider the harmonic $\frac{1}{k}$ if $(\mathbb{Z}/k\mathbb{Z})^*$ is cyclic. We define the arithmetic function, $G : \mathbb{N} \setminus \{1\} \to \mathbb{R}$ as

$$G(n) := 1 + \sum_{\substack{k=2 \\ k \text{ is cyclic}}}^{n} \frac{1}{k}$$

From these definitions, it is easy to verify that $p(n) < G(n) < g(n)$ for any $n \geq 9$. The range of n in Table 1 is scaled up intentionally to give a feel about the asymptotic behavior of these arithmetic functions. From Table 1, it is evident that the rate of growth of p is very much slower than the harmonic function and hence p is unable to give an a priori estimate of the exponential layer. From this observation it is clear that to capture the exponential layer efficiently we may expect the arithmetic function to be faster than the function p.

Now, we present a few asymptotic behavior of the proposed mesh generating function G and the arithmetic function p. In this article we have used o and Θ asymptotic notations to study the behavior of these functions and for these notations the readers may refer to [20].

Table 1 Asymptotic comparison of arithmetic functions namely g, G, g/G, p, G/p

n	$g(n)$	$G(n)$	$g(n)/G(n)$	$p(n)$	$G(n)/p(n)$
10^1	2.828968254	2.803968254	1.008915935	1.176190476	2.383940621
10^2	5.177377518	3.958820606	1.307808065	1.802817201	2.195907940
10^3	7.484470861	4.638043521	1.613712943	2.198080127	2.110042971
10^4	9.787506036	5.091117046	1.922467299	2.483059947	2.050339965
10^5	12.09013613	5.435626874	2.224239524	2.705272179	2.009271716
10^6	14.39272572	5.714779613	2.518509321	2.887328100	1.979262285
10^7	16.69531127	5.949879672	2.805991412	3.041449381	1.956264572
10^8	18.99789640	6.153004892	3.087580254	3.174975230	1.937969416
10^9	21.30048150	6.331854282	3.364019536	3.292755719	1.922965085
10^{10}	23.60306659	6.491623810	3.635926432	3.398115342	1.910360054

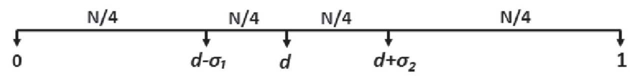

Fig. 1 Decomposition of domain to capture the interior layer

Lemma 2 *Let* $\epsilon \in \mathbb{R}^+$ *then* $G, p \in o(n^\epsilon)$

Proof The proof is straightforward since

$$G(n) - G(n-1) = \begin{cases} \frac{1}{n} & if\ (\mathbb{Z}/n\mathbb{Z})^* \ is\ cyclic, \\ 0 & otherwise \end{cases}$$

and

$$p(n) - p(n-1) = \begin{cases} \frac{1}{n} & if\ n\ is\ prime, \\ 0 & otherwise. \end{cases}$$

□

From Lemma 2, it is clear that the function G increases slower than n^ϵ for any positive constant $\epsilon \in \mathbb{R}^+$. Now, based on our observations from the Table 1 and Lemma 2 we conjecture that $G \in \Theta(p)$. In other words, the function G can be asymptotically bounded above and bounded below by constant multiples of the function p.

As said in the introduction, the solution exhibits an interior (exponential) layer at $x = d$ and we need two a priori estimates namely, σ_1 and σ_2 to estimate the width of the interior layer as shown in Figure 1. Our idea is to use the proposed function G to estimate the width of layer region and to further generate the computation mesh which is to be referred as G-mesh.

The a priori estimates for the considered class of interior layer problems are defined as

$\sigma_1 := \min\left\{\frac{d}{2}, \frac{a\epsilon}{\alpha_1}G(N)\right\}$ and

$\sigma_2 := \min\left\{\frac{1-d}{2}, \frac{a\epsilon}{\alpha_2}G(N)\right\}$

where N is the number of mesh points in the computation domain ($\overline{\Omega}^N$) and a is chosen to be a positive constant.

Now, we define the computation mesh $\overline{\Omega}^N := \{x_i \mid 0 \le i \le N\}$, where

$$x_i := \begin{cases} ih_i & for\ \ 0 \le i \le \frac{N}{4}, \\ d - \sigma_1 + \left(i - \frac{N}{4}\right)h_i & for\ \ \frac{N}{4} < i \le \frac{N}{2}, \\ d + \left(i - \frac{N}{2}\right)h_i & for\ \ \frac{N}{2} < i \le \frac{3N}{4}, \\ d + \sigma_2 + (i - \frac{3N}{4})h_i & for\ \ \frac{3N}{4} < i \le N \end{cases}$$

and

$$h_i = \begin{cases} \dfrac{4(d-\sigma_1)}{N} & for \;\; 1 \le i \le \dfrac{N}{4}, \\ \dfrac{4}{N}\sigma_1 & for \;\; \dfrac{N}{4} < i \le \dfrac{N}{2}, \\ \dfrac{4}{N}\sigma_2 & for \;\; \dfrac{N}{2} < i \le \dfrac{3N}{4}, \\ \dfrac{4(1-d-\sigma_2)}{N} & for \;\; \dfrac{3N}{4} < i \le N. \end{cases}$$

3 The analysis of upwind scheme on the proposed G-mesh

Now, we discretize the continuous problem (1) using upwind scheme on the defined computation domain ($\overline{\Omega}^N$) and it is given as,

$$\begin{aligned} L^N U_i =& \tilde{f}_i, \qquad for \;\; 1 \le i \le N-1 \\ U_0 =& u(0), \quad U_N = u(1), \end{aligned} \tag{3}$$

where

$$L^N U_i = \begin{cases} \epsilon D^+ D^- U_i + a_i D^- U_i & for \;\; 1 \le i < \dfrac{N}{2}, \\ \epsilon D^+ D^- U_i + a_i D^+ U_i & for \;\; \dfrac{N}{2} < i < N, \\ D^+ U_{\frac{N}{2}} - D^- U_{\frac{N}{2}} & for \;\; i = \dfrac{N}{2}, \end{cases}$$

$$\tilde{f}_i = \begin{cases} f_i & for \;\; 1 \le i < \dfrac{N}{2} \;\&\; \dfrac{N}{2} < i < N, \\ 0 & for \;\; i = \dfrac{N}{2}. \end{cases}$$

It is to be noted that $U_i = U(x_i)$, $f_i = f(x_i)$, $D^+ U_i = \dfrac{U_{i+1} - U_i}{h_{i+1}}$, $D^- U_i = \dfrac{U_i - U_{i-1}}{h_i}$ and

$$D^+ D^- U_i = \frac{2}{h_i h_{i+1}(h_i + h_{i+1})}(h_{i+1} U_{i-1} - (h_{i+1} + h_i) U_i + h_i U_{i+1}).$$

Some lemmas which are useful for theoretical error analysis are listed below and the readers may refer to [1] for further information.

Lemma 3 *Let the mesh function Φ satisfies, $\Phi(0) \le 0$, $\Phi(1) \le 0$ and $L^N \Phi(x_i) \ge 0$, $\forall x_i \in \Omega^N$ then $\Phi(x_i) \le 0$, $\forall x_i \in \overline{\Omega}^N$*

Lemma 4 *The bound for the solution of the discrete problem* (3) *is estimated as*

$$\|U\|_{\overline{\Omega}^N} \le max\{|u(0)|, |u(1)|\} + \frac{1}{\gamma}\|\tilde{f}\|_{\overline{\Omega}^N}$$

where $\gamma = min\left\{\dfrac{\alpha_1}{d}, \dfrac{\alpha_2}{1-d}\right\}$.

Lemma 5 *Let* $\Phi(x_i) = \begin{cases} x_i & for \; 0 \le i \le \dfrac{N}{2}, \\ 1 - x_i & for \; \dfrac{N}{2} \le i \le N, \end{cases}$ *then*

$$-L^N \Phi(x_i) > \begin{cases} \alpha_1 \; for \; 1 \le i < \dfrac{N}{2}, \\ \alpha_2 \; for \; \dfrac{N}{2} < i < N. \end{cases}$$

Theorem 1 *We have the following error estimate for the upwind scheme on G-mesh*

$$\|U - u\|_{\overline{\Omega}^N} \le CN^{-1}(G(N))^2$$

Proof Using the decomposition technique presented in [1], we decompose the solution of (3) as,

$$U_i = \begin{cases} Y_{L,i} + Z_{L,i} & for\ 1 \le i < \frac{N}{2}, \\ Y_{L,\frac{N}{2}} + Z_{L,\frac{N}{2}} = Y_{R,\frac{N}{2}} + Z_{R,\frac{N}{2}} & for\ i = \frac{N}{2}, \\ Y_{R,i} + Z_{R,i} & for\ \frac{N}{2} < i < N, \end{cases}$$

where Y_L and Y_R are chosen such that,

$$L^N Y_{L,i} = f_i \quad for\ all\ \ 1 \le i < \frac{N}{2}, Y_{L,0} = y(0),\ Y_{L,\frac{N}{2}} = y(d^-)$$
$$L^N Y_{R,i} = f_i \quad for\ all\ \frac{N}{2} < i < N, Y_{R,\frac{N}{2}} = y(d^+),\ Y_{R,N} = y(1)$$

and Z_L and Z_R are chosen such that,

$$L^N Z_{L,i} = 0\ \ for\ all\ 1 \le i < \frac{N}{2}, L^N Z_{R,i} = 0\ \ for\ all\ \frac{N}{2} < i < N,$$
$$Z_{L,0} = 0,\ Z_{R,N} = 0, Y_{L,\frac{N}{2}} + Z_{L,\frac{N}{2}} = Y_{R,\frac{N}{2}} + Z_{R,\frac{N}{2}},$$
$$D^- Y_{L,\frac{N}{2}} + D^- Z_{L,\frac{N}{2}} = D^+ Y_{R,\frac{N}{2}} + D^+ Z_{R,\frac{N}{2}}.$$

Let us estimate the error by splitting into two cases, namely outside and inside the layer region.
Case (i) (outside the layer region). The error bound for outside the layer region can be estimated by further splitting it into two cases namely y (smooth component) and z (singular component).

From [1] the error estimate, for the smooth component which is left to the layer region i.e. for $1 \le i \le \frac{N}{4}$, we have $|Y_{L,i} - y(x_i)| \le CN^{-1}$ and for the smooth component which is right to the layer region i.e. for $\frac{3N}{4} \le i \le N-1$, we have $|Y_{R,i} - y(x_i)| \le CN^{-1}$.

Now, for z (singular component) which is left to the layer region i.e. for $1 \le i \le N/4$, we have

$$|Z_{L,i} - z(x_i)| \le |Z_{L,i}| + |z(x_i)|. \tag{4}$$

Using the inequality $|Z_{L,i}| \le CN^{-1}$ for $1 \le i \le N/4$ from [1] and from Lemma 1 we get,

$$\begin{aligned} |Z_{L,i} - z(x_i)| &\le CN^{-1} + Ce^{-\alpha_1\sigma_1/\epsilon} \\ &= CN^{-1} + Ce^{-aG(N)} \\ &\le CN^{-1} + Ce^{-\ln N} \quad (a\ is\ such\ that\ \ aG(N) > \ln N) \\ &\le CN^{-1}. \end{aligned}$$

Similarly, we can prove that $|Z_{R,i} - z(x_i)| \le CN^{-1}$ for $\frac{3N}{4} \le i \le N-1$ and thus we have the following error estimate for outside the layer.

$$|U_i - u(x_i)| \le CN^{-1},\ \ for\ 1 \le i \le \frac{N}{4}\ \&\ \frac{3N}{4} \le i \le N-1 \tag{5}$$

Case (ii) (inside the layer region). From equation (5) we have

$$|U_i - u(x_i)| \le CN^{-1},\ \ for\ i = \frac{N}{4}\ and\ i = \frac{3N}{4}.$$

From [15, Lemma 3.3] and Lemma 1, for $\frac{N}{4} < i < \frac{N}{2}$ we get,

$$
\begin{aligned}
|L^N(U_i - u(x_i))| &\le Ch_i\big(\epsilon|u^{(3)}| + |u^{(2)}|\big)\\
&\le Ch_i\epsilon^{-2}e^{-\alpha_1(d-x_i)/\epsilon}\\
&\le Ch_i\epsilon^{-2} \quad (\because x_i \in (d-\sigma_1, d])\\
&\le CN^{-1}\sigma_1\epsilon^{-2}.
\end{aligned}
$$

Similarly, for $\frac{N}{2} < i \le \frac{3N}{4}$,

$$|L^N(U_i - u(x_i))| \le CN^{-1}\sigma_2\epsilon^{-2}.$$

For $i = \frac{N}{2}$, from [16] we have the inequalities $|u'(x_i) - D^+u(x_i)| \le \frac{(x_{i+1}-x_i)|u_i^{(2)}|}{2}$ and $|u'(x_i) - D^-u(x_i)| \le \frac{(x_i - x_{i-1})|u_i^{(2)}|}{2}$ and thus,

$$
\begin{aligned}
|(D^+ - D^-)(U_i - u(x_i))| &= |(D^- - D^+)u(x_i) + [u'(x_i)]|\\
&\le |u'(x_i) - D^+u(x_i)| + |u'(x_i) - D^-u(x_i)|\\
&\le \frac{h_{i+1}|u_i^{(2)}|}{2} + \frac{h_i|u_i^{(2)}|}{2}\\
&\le C(h_{i+1}+h_i)\epsilon^{-2}e^{-(d-x_i)\alpha_1/\epsilon} \ (from\ Lemma\ 1)\\
&\le C(h_{i+1}+h_i)\epsilon^{-2}\\
&= CN^{-1}\sigma_1\epsilon^{-2} + CN^{-1}\sigma_2\epsilon^{-2}
\end{aligned}
$$

Now, let us define a mesh function $\psi \pm (U-u)$ on $\overline{\Omega}^N \cap [d-\sigma_1, d+\sigma_2]$, where

$$
\psi = -CN^{-1} - \begin{cases} C\frac{N^{-1}\sigma_1}{\epsilon^2}(x_i - (d-\sigma_1)) \\ \quad for\ \frac{N}{4} \le i \le \frac{N}{2}, \\ C\frac{N^{-1}\sigma_2}{\epsilon^2}((d+\sigma_2) - x_i) \\ \quad for\ \frac{N}{2}+1 \le i \le \frac{3N}{4}. \end{cases}
$$

Then by applying Lemma 3 to the above defined mesh function we get,

$$|U_i - u(x_i)| \le CN^{-1}(G(N))^2,\ for\ \frac{N}{4} < i < \frac{3N}{4}. \tag{6}$$

From Equations (5) and (6), the result follows. □

4 Numerical results

In this section, we present a few numerical experiments supporting the theoretical estimates proved in Section 3. We consider the following two numerical examples from the considered class of problems to demonstrate the efficiency of the proposed G-mesh.

Example 1

$$
\begin{aligned}
\epsilon u''(x) + a(x)u'(x) &= f(x), \quad x \in (0, 0.5) \cup (0.5, 1),\\
u(0) = 0, &\quad u(1) = 0,
\end{aligned}
$$

where

$$
a(x) = \begin{cases} -(2-x) & 0 \le x \le 0.5,\\ 2 & otherwise, \end{cases}
$$

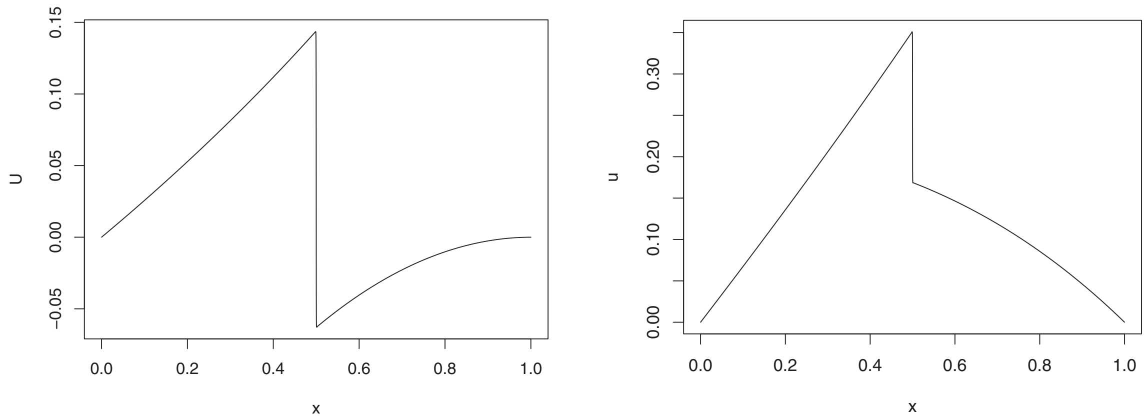

(a) Example 1 (b) Example 2

Fig. 2 Numerical solution computed using upwind scheme on G-mesh for $\epsilon = 2^{-12}$ and $N = 512$.

and

$$f(x) = \begin{cases} -0.5 & 0 \leq x \leq 0.5, \\ 1 - x & otherwise. \end{cases}$$

Example 2

$$\begin{gathered} \epsilon u''(x) + a(x)u'(x) = f(x), \quad x \in (0, 0.5) \cup (0.5, 1), \\ u(0) = 0, \quad u(1) = 0, \end{gathered}$$

where

$$a(x) = \begin{cases} -(3 - 2x) & 0 \leq x \leq 0.5, \\ 3 - x & otherwise, \end{cases}$$

and

$$f(x) = \begin{cases} -(2 - x) & 0 \leq x \leq 0.5, \\ -x & otherwise. \end{cases}$$

The exact solution of these examples are not known, so we estimate the errors using double mesh principle [17,18]. The maximum point-wise error (E_ϵ^N) and the parameter uniform error (E^N) are estimated by

$$E_\epsilon^N = \max_{0 \leq i \leq N} \{|u(x_i) - U_i|\} \ \ and \ \ E^N = \max_\epsilon \{E_\epsilon^N\}$$

Similarly, the numerical rate of convergence (P_ϵ^N) and the parameter uniform rate of convergence (P^N) are estimated using

$$P_\epsilon^N = \log_2\left(\frac{E_\epsilon^N}{E_\epsilon^{2N}}\right) \ \ and \qquad P^N = \log_2\left(\frac{E^N}{E^{2N}}\right)$$

The numerical solutions of Examples 1 and 2 using upwind scheme on G-mesh (with $\epsilon = 2^{-12}$, $N = 512$) are shown in Figures (2a) and (2b) respectively. Similarly the point-wise error of these solutions are shown in Figure (3a) and (3b) respectively. It is to be observed that the maximum error occurs in the neighborhood of the point of discontinuity, namely $x = 0.5$ as discussed in Section 3.

Tables 2 and 3 shows that the upwind scheme on the proposed G-mesh is ϵ-uniformly convergent and the rate of convergence is almost first order. In order to benchmark the performance of the proposed G-mesh, we present Tables 4 and 5 comparing the respective maximum point-wise error (E_ϵ^N) and the numerical rate of convergence (P_ϵ^N) of Examples 1 and 2 computed using the standard upwind scheme on harmonic, Shishkin, the proposed G-mesh and B-type meshes. It is evident from these tables that G-mesh is able to give more accurate results

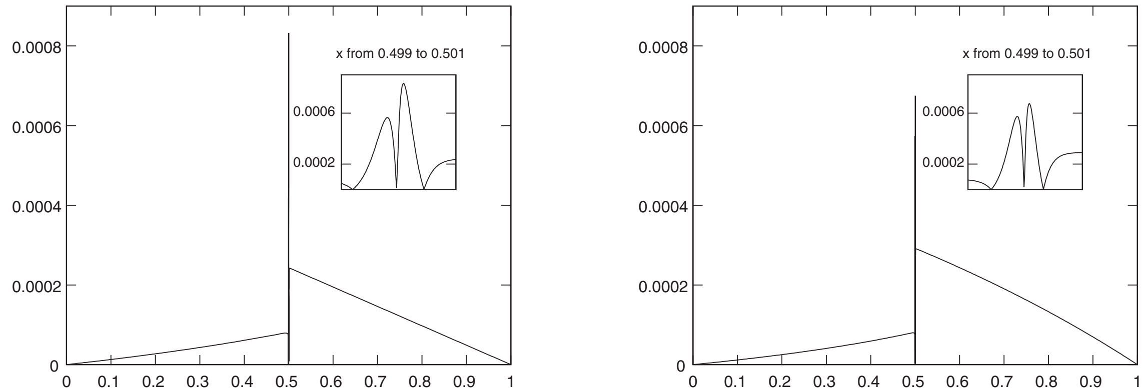

(a) Example 1 (b) Example 2

Fig. 3 Point-wise error computed using upwind scheme on G-mesh for $\epsilon = 2^{-12}$ and $N = 512$.

Table 2 E_ϵ^N, E^N and P^N for Example 1 using upwind scheme on G-mesh

ϵ / N	32	64	128	256	512	1,024	2,048	4,096
2^{-6}	5.3481E-03	3.9166E-03	2.6369E-03	1.5868E-03	8.9312E-04	4.8410E-04	2.5614E-04	1.3365E-04
2^{-7}	5.0882E-03	3.7580E-03	2.5430E-03	1.5340E-03	8.6590E-04	4.6982E-04	2.4881E-04	1.2992E-04
2^{-8}	5.0764E-03	3.6642E-03	2.4873E-03	1.5026E-03	8.4962E-04	4.6139E-04	2.4443E-04	1.2768E-04
2^{-9}	5.0706E-03	3.6137E-03	2.4571E-03	1.4856E-03	8.4074E-04	4.5677E-04	2.4204E-04	1.2644E-04
2^{-10}	5.0676E-03	3.5876E-03	2.4415E-03	1.4767E-03	8.3611E-04	4.5434E-04	2.4076E-04	1.2578E-04
2^{-11}	5.0660E-03	3.5744E-03	2.4337E-03	1.4723E-03	8.3380E-04	4.5312E-04	2.4011E-04	1.2543E-04
2^{-12}	5.0652E-03	3.5677E-03	2.4297E-03	1.4700E-03	8.3266E-04	4.5254E-04	2.3980E-04	1.2525E-04
2^{-13}	5.0648E-03	3.5643E-03	2.4277E-03	1.4689E-03	8.3211E-04	4.5227E-04	2.3967E-04	1.2517E-04
2^{-14}	5.0646E-03	3.5627E-03	2.4267E-03	1.4684E-03	8.3183E-04	4.5215E-04	2.3962E-04	1.2516E-04
2^{-15}	5.0645E-03	3.5618E-03	2.4262E-03	1.4681E-03	8.3170E-04	4.5209E-04	2.3960E-04	1.2516E-04
2^{-16}	5.0644E-03	3.5614E-03	2.4260E-03	1.4680E-03	8.3163E-04	4.5206E-04	2.3960E-04	1.2517E-04
2^{-17}	5.0644E-03	3.5612E-03	2.4258E-03	1.4679E-03	8.3160E-04	4.5205E-04	2.3959E-04	1.2518E-04
2^{-18}	5.0644E-03	3.5611E-03	2.4258E-03	1.4679E-03	8.3158E-04	4.5204E-04	2.3959E-04	1.2518E-04
2^{-19}	5.0644E-03	3.5610E-03	2.4257E-03	1.4678E-03	8.3157E-04	4.5203E-04	2.3959E-04	1.2518E-04
2^{-20}	5.0644E-03	3.5610E-03	2.4257E-03	1.4678E-03	8.3157E-04	4.5203E-04	2.3959E-04	1.2518E-04
E^N	5.3481E-03	3.9166E-03	2.6369E-03	1.5868E-03	8.9312E-04	4.8410E-04	2.5614E-04	1.3365E-04
P^N	0.4494	0.5707	0.7327	0.8291	0.8835	0.9183	0.9384	-

when compared with Shishkin or harmonic meshes. It is also to be noted that B-type mesh is giving better results when compared to these meshes and when it comes to reduction to practice B-type mesh has its own complexity due to the nature of non-uniformity in the layer region. From Tables 6 and 7, it is evident that one can achieve 40-50% efficiency by using the proposed G-mesh when compared with other piecewise uniform meshes namely, Shishkin or harmonic meshes. It is also evident from these tables that one can achieve 70% efficiency by using the non-uniform B-type mesh when compared with Shishkin or harmonic meshes. Therefore from these numerical experiments one can infer that among the piecewise uniform meshes the proposed G-mesh is more efficient and also ease of use when compared with non-uniform B-type mesh. It is also to be noted that one can generalize the proposed G-mesh like the one generalized by Vulanovic namely the $S(\ell)$ mesh [19]. In future we will also try to tackle singularly perturbed problems through variable resolution spectral methods and G-mesh [22].

Table 3 E_ϵ^N, E^N and P^N for Example 2 using upwind scheme on G-mesh

ϵ / N	32	64	128	256	512	1,024	2,048	4,096
2^{-6}	6.3559E-03	3.8744E-03	2.2206E-03	1.2328E-03	6.6213E-04	3.5535E-04	1.8937E-04	9.9303E-05
2^{-7}	5.7701E-03	3.5682E-03	2.0642E-03	1.1565E-03	6.6291E-04	3.6310E-04	1.9343E-04	1.0141E-04
2^{-8}	5.4746E-03	3.4124E-03	1.9840E-03	1.1700E-03	6.6890E-04	3.6659E-04	1.9517E-04	1.0230E-04
2^{-9}	5.3258E-03	3.3336E-03	1.9432E-03	1.1758E-03	6.7229E-04	3.6808E-04	1.9593E-04	1.0271E-04
2^{-10}	5.2511E-03	3.2938E-03	1.9225E-03	1.1785E-03	6.7386E-04	3.6876E-04	1.9631E-04	1.0289E-04
2^{-11}	5.2136E-03	3.2739E-03	1.9120E-03	1.1798E-03	6.7463E-04	3.6908E-04	1.9649E-04	1.0298E-04
2^{-12}	5.1949E-03	3.2639E-03	1.9125E-03	1.1805E-03	6.7501E-04	3.6925E-04	1.9659E-04	1.0302E-04
2^{-13}	5.1855E-03	3.2589E-03	1.9133E-03	1.1808E-03	6.7520E-04	3.6934E-04	1.9664E-04	1.0305E-04
2^{-14}	5.1808E-03	3.2564E-03	1.9138E-03	1.1810E-03	6.7530E-04	3.6938E-04	1.9667E-04	1.0307E-04
2^{-15}	5.1785E-03	3.2551E-03	1.9140E-03	1.1811E-03	6.7535E-04	3.6941E-04	1.9669E-04	1.0308E-04
2^{-16}	5.1773E-03	3.2545E-03	1.9141E-03	1.1811E-03	6.7537E-04	3.6942E-04	1.9670E-04	1.0309E-04
2^{-17}	5.1767E-03	3.2542E-03	1.9142E-03	1.1811E-03	6.7539E-04	3.6942E-04	1.9670E-04	1.0309E-04
2^{-18}	5.1764E-03	3.2540E-03	1.9142E-03	1.1811E-03	6.7539E-04	3.6943E-04	1.9670E-04	1.0309E-04
2^{-19}	5.1763E-03	3.2539E-03	1.9142E-03	1.1811E-03	6.7540E-04	3.6943E-04	1.9671E-04	1.0309E-04
2^{-20}	5.1762E-03	3.2539E-03	1.9142E-03	1.1811E-03	6.7540E-04	3.6943E-04	1.9671E-04	1.0309E-04
E^N	6.3559E-03	3.8744E-03	2.2206E-03	1.2328E-03	6.7540E-04	3.6943E-04	1.9671E-04	1.0309E-04
P^N	0.7141	0.8030	0.8490	0.8681	0.8704	0.9092	0.9320	-

Table 4 Comparing E_ϵ^N and P_ϵ^N of upwind scheme on harmonic, Shishkin, the proposed G-mesh and B-type meshes for Example 1

ϵ	N	Harmonic mesh (E_H)	Shishkin mesh (E_S)	G-mesh (proposed) (E_G)	B-type mesh (E_B)
2^{-10}	32	5.7176E-03	5.0479E-03	5.0676E-03	6.9154E-03
		(0.3646)	(0.3593)	(0.4982)	(0.8446)
	64	4.4407E-03	3.9348E-03	3.5876E-03	3.8508E-03
		(0.4603)	(0.4282)	(0.5552)	(0.9265)
	128	3.2274E-03	2.9243E-03	2.4415E-03	2.0259E-03
		(0.5926)	(0.5904)	(0.7253)	(0.9634)
	256	2.1401E-03	1.9421E-03	1.4767E-03	1.0390E-03
		(0.7007)	(0.6924)	(0.8206)	(0.9816)
	512	1.3167E-03	1.2017E-03	8.3611E-04	5.2616E-04
		(0.7718)	(0.7606)	(0.8799)	(0.9907)
	1024	7.7120E-04	7.0932E-04	4.5434E-04	2.6477E-04
		(0.8167)	(0.8085)	(0.9161)	(0.9952)
	2048	4.3783E-04	4.0499E-04	2.4076E-04	1.3282E-04
		(0.8485)	(0.8399)	(0.9366)	(0.9976)
	4096	2.4315E-04	2.2625E-04	1.2578E-04	6.6521E-05
2^{-20}	2	5.7104E-03	5.0448E-03	5.0644E-03	6.9928E-03
		(0.3737)	(0.3692)	(0.5081)	(0.8666)
	64	4.4070E-03	3.9055E-03	3.5610E-03	3.8350E-03
		(0.4593)	(0.4271)	(0.5538)	(0.9317)
	128	3.2052E-03	2.9047E-03	2.4257E-03	2.0103E-03
		(0.5911)	(0.5890)	(0.7247)	(0.9640)
	256	2.1276E-03	1.9310E-03	1.4678E-03	1.0305E-03
		(0.6999)	(0.6917)	(0.8197)	(0.9816)
	512	1.3097E-03	1.1954E-03	8.3157E-04	5.2186E-04
		(0.7714)	(0.7603)	(0.8794)	(0.9909)
	1024	7.6725E-04	7.0574E-04	4.5203E-04	2.6258E-04
		(0.8162)	(0.8082)	(0.9158)	(0.9954)
	2048	4.3572E-04	4.0302E-04	2.3959E-04	1.3170E-04
		(0.8483)	(0.8398)	(0.9365)	(0.9976)
	4096	2.4199E-04	2.2517E-04	1.2518E-04	6.5957E-05

Table 5 Comparing E_ϵ^N and P_ϵ^N of upwind scheme on harmonic, Shishkin, the proposed G-mesh and B-type meshes for Example 2

ϵ	N	Harmonic mesh (E_H)	Shishkin mesh (E_S)	G-mesh (proposed) (E_G)	B-type mesh (E_B)
2^{-10}	32	5.7982E-03 (0.5870)	5.2342E-03 (0.5671)	5.2511E-03 (0.6728)	6.2610E-03 (0.8773)
	64	3.8599E-03 (0.5688)	3.5327E-03 (0.5979)	3.2938E-03 (0.7768)	3.4083E-03 (0.9387)
	128	2.6022E-03 (0.5641)	2.3340E-03 (0.5599)	1.9225E-03 (0.7059)	1.7781E-03 (0.9638)
	256	1.7599E-03 (0.6838)	1.5832E-03 (0.6736)	1.1785E-03 (0.8064)	9.1162E-04 (0.9814)
	512	1.0956E-03 (0.7594)	9.9259E-04 (0.7453)	6.7386E-04 (0.8697)	4.6171E-04 (0.9905)
	1,024	6.4719E-04 (0.8097)	5.9209E-04 (0.7986)	3.6876E-04 (0.9095)	2.3237E-04 (0.9952)
	2,048	3.6922E-04 (0.8097)	3.4039E-04 (0.8334)	1.9631E-04 (0.9320)	1.1657E-04 (0.9976)
	4,096	2.0585E-04	1.9102E-04	1.0289E-04	5.8381E-05
2^{-20}	32	5.7131E-03 (0.5833)	5.1597E-03 (0.5640)	5.1762E-03 (0.6697)	6.2540E-03 (0.8895)
	64	3.8130E-03 (0.5481)	3.4899E-03 (0.5764)	3.2539E-03 (0.7654)	3.3758E-03 (0.9384)
	128	2.6077E-03 (0.5640)	2.3404E-03 (0.5599)	1.9142E-03 (0.6965)	1.7614E-03 (0.9649)
	256	1.7638E-03 (0.6840)	1.5876E-03 (0.6739)	1.1811E-03 (0.8063)	9.0235E-04 (0.9820)
	512	1.0978E-03 (0.7599)	9.9506E-04 (0.7467)	6.7540E-04 (0.8704)	4.5683E-04 (0.9909)
	1,024	6.4832E-04 (0.8097)	5.9302E-04 (0.7983)	3.6943E-04 (0.9092)	2.2984E-04 (0.9954)
	2,048	3.6986E-04 (0.8429)	3.4099E-04 (0.8334)	1.9671E-04 (0.9321)	1.1528E-04 (0.9976)
	4,096	2.0620E-04	1.9135E-04	1.0309E-04	5.7735E-05

Table 6 Efficiency metric: Relative error for Example 1 using upwind scheme on various meshes

ϵ	N	Comparing piecewise uniform meshes (Harmonic and Shishkin vs G-mesh)		Comparing non-uniform mesh with piecewise uniform meshes (B-type vs Harmonic, Shishkin and G-mesh)		
		$\frac{E_H - E_G}{E_H}$ (%)	$\frac{E_S - E_G}{E_S}$ (%)	$\frac{E_H - E_B}{E_H}$ (%)	$\frac{E_S - E_B}{E_S}$ (%)	$\frac{E_G - E_B}{E_G}$ (%)
2^{-10}	32	11.37	−0.39	−20.95	−37.00	−36.46
	64	19.21	8.82	13.28	2.13	−7.34
	128	24.35	16.51	37.23	30.72	17.02
	256	31.00	23.96	51.45	46.50	29.64
	512	36.50	30.42	60.04	56.22	37.07
	1,024	41.09	35.95	65.67	62.67	41.72
	2,048	45.01	40.55	69.66	67.20	44.83
	4,096	48.27	44.41	72.64	70.60	47.11
2^{-20}	32	11.31	−0.39	−22.46	−38.61	−38.08
	64	19.20	8.82	12.98	1.81	−7.69
	128	24.32	16.49	37.28	30.79	17.12
	256	31.01	23.99	51.57	46.63	29.79
	512	36.51	30.44	60.15	56.34	37.24
	1,024	41.08	35.95	65.78	62.79	41.91
	2,048	45.01	40.55	69.77	67.32	45.03
	4,096	48.27	44.41	72.74	70.71	47.31

Table 7 Efficiency metric: Relative error for Example 2 using upwind scheme on various meshes

ϵ	N	Comparing piecewise uniform meshes (Harmonic and Shishkin vs G-mesh)		Comparing non-uniform mesh with piecewise uniform meshes (B-type vs Harmonic, Shishkin and G-mesh)		
		$\frac{E_H - E_G}{E_H}$ (%)	$\frac{E_S - E_G}{E_S}$ (%)	$\frac{E_H - E_B}{E_H}$ (%)	$\frac{E_S - E_B}{E_S}$ (%)	$\frac{E_G - E_B}{E_G}$ (%)
2^{-10}	32	9.44	−0.32	−7.98	−19.62	−19.23
	64	14.67	6.76	11.70	3.52	−3.48
	128	26.12	17.63	31.67	23.82	7.51
	256	33.04	25.56	48.20	42.42	22.65
	512	38.49	32.11	57.86	53.48	31.48
	1,024	43.02	37.72	64.10	60.75	36.99
	2,048	46.83	42.33	68.43	65.75	40.62
	4,096	50.02	46.14	71.64	69.44	43.26
2^{-20}	32	9.40	−0.32	−9.47	−21.21	−20.82
	64	14.66	6.76	11.47	3.27	−3.75
	128	26.59	18.21	32.45	24.74	7.98
	256	33.04	25.60	48.84	43.16	23.60
	512	38.48	32.12	58.39	54.09	32.36
	1,024	43.02	37.70	64.55	61.24	37.79
	2,048	46.82	42.31	68.83	66.19	41.40
	4,096	50.00	46.12	72.00	69.83	44.00

Acknowledgements We thank the referee and the editor for all their comments and suggestions to improve the presentation.

References

1. Farrell, P.A., Hegarty, A.F., Miller, J.J.H., O'Riordan, E., Shishkin, G.I.: Global maximum norm parameter-uniform numerical method for a singularly perturbed convection- diffusion problem with discontinuous convection coefficient. Mathematical and Computer Modelling 40(11), 1375-1392 (2004)
2. Farrell, P.A., Hegarty, A.F., Miller, J.J.H., O'Riordan, E., Shishkin, G.I.: Singularly perturbed convection–diffusion problems with boundary and weak interior layers. Journal of Computational and Applied Mathematics, 166(1), 133-151 (2004)
3. O'Riordan, E., Shishkin, G.I.: Singularly perturbed parabolic problems with non-smooth data. Journal of computational and applied mathematics 166.1, 233-245 (2004)
4. Cen, Z.: A hybrid difference scheme for a singularly perturbed convection-diffusion problem with discontinuous convection coefficient. Applied mathematics and computation, 169(1), 689-699 (2005)
5. Mukherjee, K., Natesan, S.: ϵ-Uniform error estimate of hybrid numerical scheme for singularly perturbed parabolic problems with interior layers. Numerical Algorithms, 58(1), 103-141 (2011)
6. Rai, P., Sharma, K.K.: Parameter uniform numerical method for singularly perturbed differential-difference equations with interior layers. International Journal of Computer Mathematics, 88(16), 3416-3435 (2011)
7. Cen, Z., Le, A., Xu, A.: A high-order finite difference scheme for a singularly perturbed reaction-diffusion problem with an interior layer. Advances in Difference equations, (1), 1-14 (2017)
8. Ramesh, V.P., Kadalbajoo, M.K., Priyanga, B., Prithvi, M.: An a priori harmonic mesh for singularly perturbed boundary value problems. International Journal of Applied and Computational Mathematics 4(6), 139 (2018)
9. Ramesh, V.P., Kadalbajoo, M.K., Prithvi, M., Priyanga, B.: Exponentially refined mesh for singularly perturbed interior layer problem. International Journal of Applied and Computational Mathematics 6(82) (2020)
10. Rai, P., Sharma, K.K.: Numerical approximation for a class of singularly perturbed delay differential equations with boundary and interior layer(s). Numerical Algorithms, 85(1), 305-328 (2020)
11. Vulanovic, R.: On a numerical solution of a type of singularly perturbed boundary value problem by using a special discretization mesh. Univ. u Novom Sadu, Zb. Rad. Prirod.-Mat. Fak., Ser. Mat 13, 187-201 (1983)
12. Bakhvalov, NS, .:Towards optimization of methods for solving boundary value problems in the presence of boundary layers. Zh. Vychisl. Mat. i Mat. Fiz. [in Russian], 841-859 (1969)
13. Shishkin, G.I.: Grid approximation of singularly perturbed elliptic and parabolic equations, second doctoral thesis. Keldysh Institute, Moscow (1990) (in Russian)
14. Linß, T.: Layer-Adapted Meshes for Reaction–Convection–Diffusion Problems. Lecture Notes in Mathematics, vol. 1985. Springer, Berlin (2010)
15. Kellogg, R.B., Tsan, A.: Analysis of some difference approximations for a singular perturbation problem without turning points. Mathematics of Computation 32(144), 1025- 1039 (1978)
16. Miller, J.J.H., O'Riordan, E., Shishkin, G.I.: Fitted Numerical Methods for Singular Perturbation Problems. World Scientific, Singapore (1996)

17. Doolan, E.P., Miller, J.J.H., Schilders, W. H.: Uniform numerical methods for problems with initial and boundary layers. Boole Press (1980)
18. Farrell, P.A., Hegarty, A.F.: On the determination of the order of uniform convergence. In Proceedings of IMACS, 91, 501-502 (1991)
19. Vulanovic, R.: A priori meshes for singularly perturbed quasilinear two-point boundary value problems. IMA Journal of Numerical Analysis 21(1), 349-366 (2001)
20. Ramesh, V.P., Gowtham R.: Asymptotic Notations and its Applications, The Ramanujan Mathematical Society: Mathematics Newsletter, 28(4), 10-16 (2017)
21. Ramesh, V.P., Thangadurai, R., Thatchaayini, R.: A Note on Gauss's Theorem on Primitive Roots. The American Mathematical Monthly, 126(3), 252-254 (2019)
22. Janakiraman S., Nanjundiah Ravi S., Vasudeva Murthy A.S. ,: A novel variable resolution global spectral method on the sphere, Journal of Computational Physics, 231(7), 2794-2810, (2012)